Histamine H_3 Receptor Function Biases Excitatory Gain in the Nucleus Accumbens

Supplemental Information

Supplemental Figures

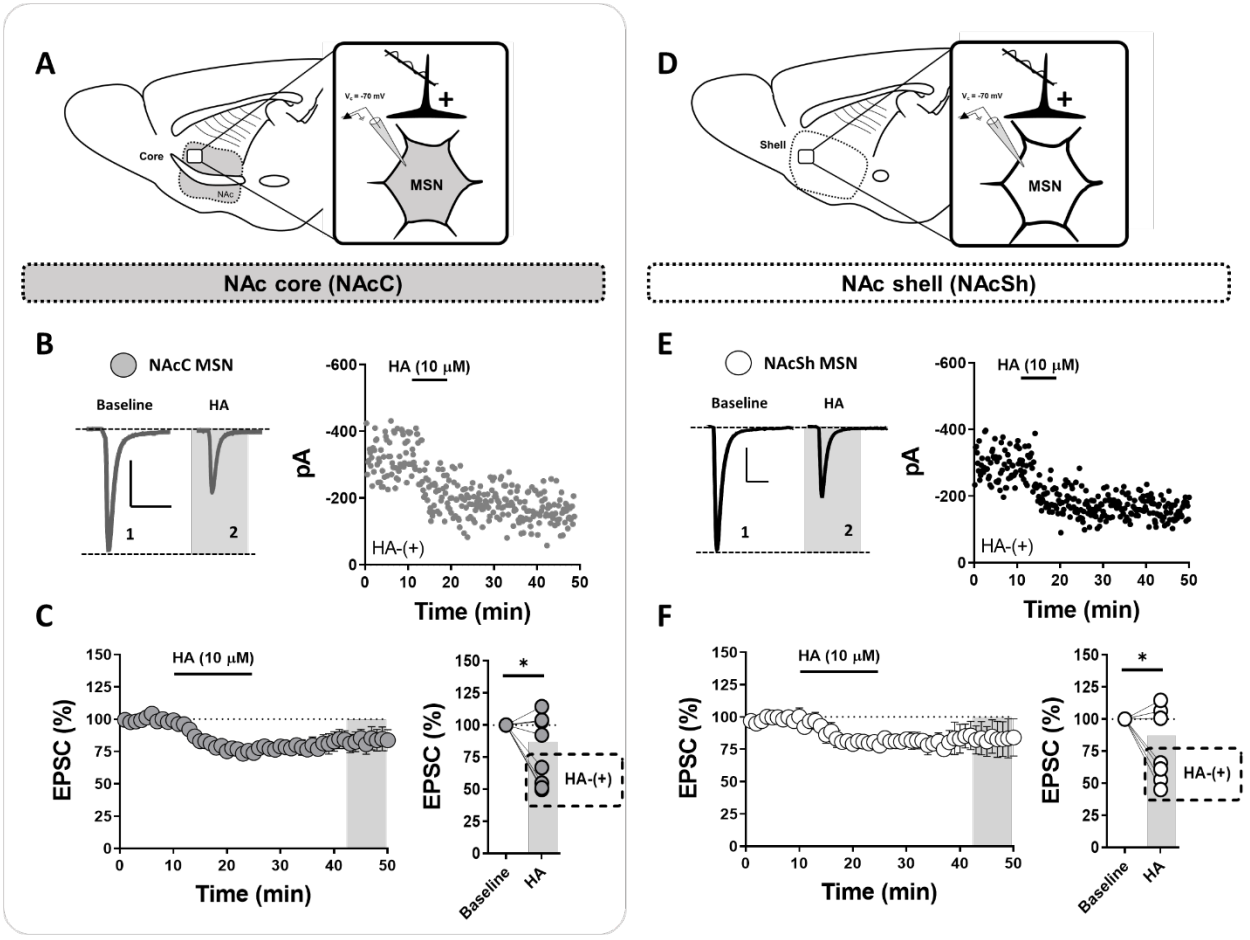

Figure S1. Histamine decreases glutamatergic transmission onto MSNs in the NAc core and shell. (A) Schematic of sagittal C57Bl/6 WT mouse brain slice depicting recording area and electrophysiological configuration in the dorsomedial NAc core (grey). **(B)** Representative traces and experiment of EPSCs obtained from unlabeled MSNs at -70 mV in the NAc core following bath-application of HA. **(C)** Time-course summary and average EPSC amplitude obtained t(grey) = 45-50-min following HA application in the NAc core [79.46±10.08%, n=8, p=0.033]. **(D)** Schematic of sagittal C57Bl/6 WT mouse brain slice depicting recording area and electrophysiological configuration in the medial NAc shell (white). **(E)** Representative traces and experiment of EPSCs obtained from unlabeled MSNs at -70 mV in the NAc shell following bath-application of HA. **(F)** Time-course summary and average EPSC amplitude obtained t(grey) = 45-50-min following HA application in the NAc shell [78.01±11.57%, n=7, p=0.043]. Scale bars: 100-pA/50-ms. *Note:* highlighted "HA-(+)" cells in bar graph summary indicate cells that underwent a clear depression (>10-15%) in EPSC amplitude. Error bars indicate SEM with (*) signifying $p < 0.05$.

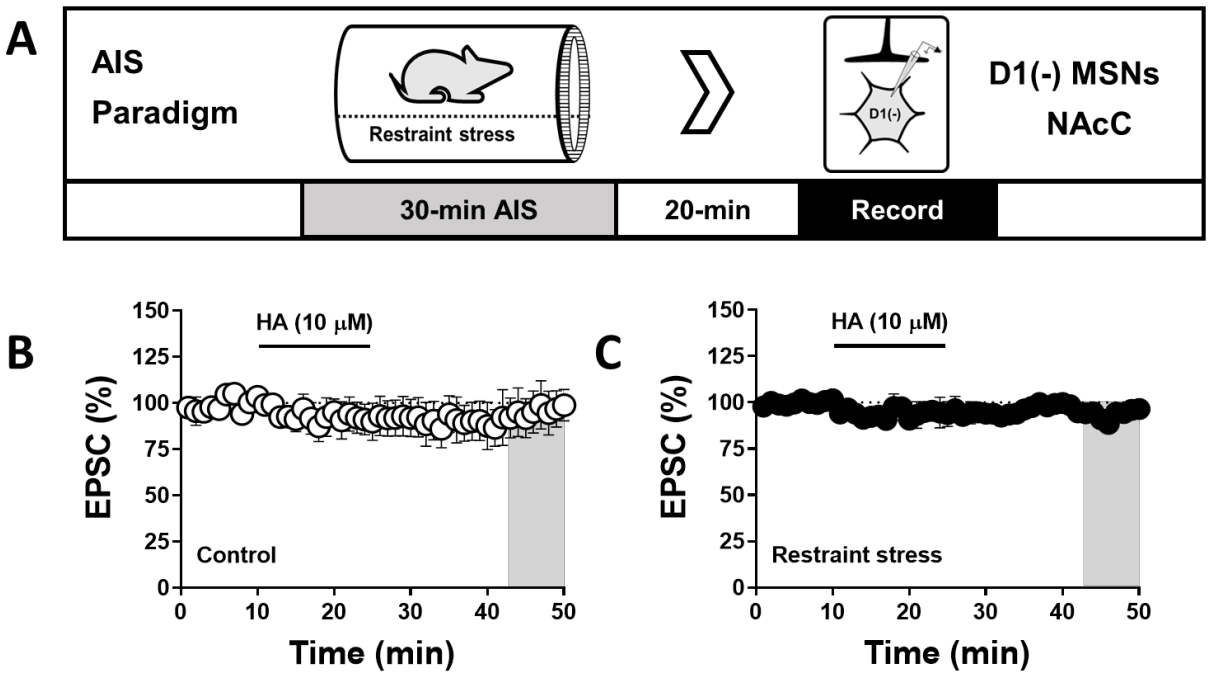

Figure S2. Acute immobilization stress does not reveal HA-induced effects at glutamatergic synapses onto D1(-) MSNs in the NAc core. (A) Schematic depicting 30-min acute immobilization stress (AIS) paradigm and recording strategy in D1(-) MSNs of control (open circles) and AIS-exposed D1tdTomato mice (black circles). **(B)** Time-course summary of EPSCs in control homecage mice during HA application at synapses onto D1(-) MSNs. **(C)** Time-course summary of EPSCs in AIS-exposed mice during HA application at synapses onto D1(-) MSNs [HA control: 97.69±7.22%, n=5, N(animals)=3, p=0.0932; HA AIS: 94.45±2.22%, n=4, N(animals)=3]. Error bars indicate SEM with (*) signifying $p < 0.05$.

Supplemental Methods and Materials

Animals

Animals were bred and housed at Vanderbilt University Medical Center in accordance with IACUC. Male mice 8-12 weeks of age were used for all electrophysiological and *in vivo* experiments. Mice were housed in groups of 3-5/cage on a 12-hr light-dark cycle with *ad lib* access to standard food and water. Breeding cages were given 5LOD chow (PicoLab ®, 28.7% protein, 13.4 % fat, 57.9 % carbohydrate) to improve litter viability. Electrophysiology experiments were performed in either C57BL/6J wild-type (WT) mice (no MSN subtype-specificity) or WT mice bred to harbor a bacterial artificial chromosome (BAC) carrying the tdTomato fluorophore under control of the *Drd1a* (D1 receptor) promoter (B6.Cg-Tg(Drd1a-tdTomato)6Calak/J, Stock No: 016204, Jackson labs). For a subset of experiments, mice underwent closely monitored 30-min acute immobilization stress (AIS) in an aerated cylindrical holding tube followed by a 20-min recovery period. "Control" mice were kept in their homecage prior to slice electrophysiology recordings.

Electrophysiology

Whole-cell patch-clamp electrophysiological recordings were obtained in acute brain slice preparations from C57BL/6J WT mice or D1tdTomato BAC transgenic mice. Mice were euthanized under isoflurane anesthesia and decapitated, after which parasagittal slices (250 μm) containing the NAc core and shell were prepared from whole brain tissue using a Leica Vibratome in oxygenated (95% O2; 5%CO2) ice-cold *N*-methyl-*D*-glucamine (NMDG)-based solution (in mM: 2.5 KCl, 20 HEPES, 1.2 NaH_2PO_4, 25 Glucose, 93 NMDG, 30 $NaHCO_3$, 5.0 sodium ascorbate, 3.0 sodium pyruvate, 10 $MgCl_2$, and 0.5 $CaCl_2$-$2H_2O$). Slices were then recovered in NMDG-based recovery solution for 10-15-min at 31-32 °C before being transferred to a chamber containing artificial cerebral spinal fluid (ACSF, in mM: 119 NaCl, 2.5 KCl, 1.3 $MgCl_2$-$6H_2O$, 2.5 $CaCl_2$-$2H_2O$, 1.0 NaH_2PO4-H_2O, 26.2 $NaHCO_3$, and 11 glucose; 287-295 mOsm). All electrophysiology experiments were performed using a Scientifica Slicescope Pro System with continuously-perfused 28-32 °C ACSF at 2 mL/min. MSNs in the NAc were visualized using Scientifica PatchVision software and patched with 3–6 MΩ recording pipettes (P1000 Micropipette Puller) filled with K^+-based intracellular solution: (in mM: 135 K^+-gluconate, 5 NaCl, 2 $MgCl_2$, 10 HEPES, 0.6 EGTA, 3 Na_2ATP, 0.4 Na_2GTP; 290 mOsm). D1(+) and D1(-)

(putative D2) MSNs were differentiated according to the expression of the tdTomato fluorophore stimulated via 530 nm LED light. D1(-) MSNs were distinguished from interneuron cell types based on morphological (size, shape) and biophysical properties (e.g., capacitance, membrane resistance, and AMPAR-mediated EPSC rise time and decay kinetics).

For *voltage-clamp* recordings, electrically-evoked excitatory postsynaptic currents (eEPSCs) were obtained at a command voltage of -70 mV and isolated with $GABA_AR$ antagonist, picrotoxin (PTX, 50 μM), into the ACSF bath. In experiments examining local glutamatergic transmission, a bipolar electrode was placed at the corticoaccumbens interface and stimulated at 0.1 Hz. The NAc core (NAcC) was differentiated from the NAc shell (NAcSh) according to established anatomical landmarks, including the anteroposterior communication of the anterior commissure. In mice stereotaxically injected with ChR2 in the PFC or MDT, optically-evoked glutamate release was sampled with a 0.3-0.5-ms stimulus duration at 10-30% stimulus intensity. Paired pulse ratios (PPR) were obtained within-experiment by delivering two 0.3-ms duration pulses with a 50-ms interstimulus interval and calculating the amplitude ratio of the second eEPSC to the first eEPSC ($eEPSC_2/eEPSC_1$) at the indicated time-point. Coefficient of variance (CV) analysis was conducted within-experiment by calculating σ/μ of PSC amplitudes before and after drug exposure. sEPSC analysis was performed with Clampfit 10.4 using a best-fit template obtained from preliminary 10-min recording bouts in D1(+) and D1(-) MSNs. Each recording bout yielded a rise time ($\leq$ 3-ms) and amplitude ($\geq$ 5 pA) selection criteria that was reflected in the overall template score. RuBi-Glu experiments were obtained by field-illumination with 470 nm LED blue light with a 60-sec ISI and baseline RuBi-Glu oEPSC between 40-70 pA.

For *current-clamp* recordings, cells were permitted to equilibrate to the intracellular dialysate for 5-min after entering whole-cell configuration, after which a depolarizing plateau potential was established to maintain cells between -65 and -70 mV. Synaptically-evoked action potential (AP) fidelity was assessed by first obtaining 15-20 mV EPSP amplitudes at resting membrane potential to permit between-cell analyses. A bipolar stimulating electrode was placed between 100-200 μm from cells to prevent non-synaptic AP volleys. 12-15 stimulus trains were delivered at frequencies of 1, 5, 10, 20 and 30 Hz with a stimulus duration of 0.1 ms. AMPAR-mediated AP firing was confirmed by performing this protocol in the presence of AMPAR antagonist, NBQX. Membrane

resistance and series resistance (R_S) were monitored continuously during all experiments, with >15-20% change resulting in the omission of that experiment.

Stereotaxic surgery

4–6-week-old male D1tdTomato mice were anesthetized using ketamine (75 mg/kg I.P.) and dexdomitidor (0.5 mg/kg I.P.). Craniotomies were performed using a drill, AmScope microscope, and World Precision Instruments Aladdin Al-2000 syringe pump hydraulic system. The following coordinates were used based on The Mouse Brain in Stereotaxic Coordinates: PFC (AP 1.4, ML ± 0.5, DV −2.9 mm) and MDT (AP −1.2, ML 0.3, DV −3.00 mm). Injection sites were located using Leica AngleTwo Stereotaxic software. AAV-CaMKII-ChR2-eYFP (Addgene) was injected at 100 nL/min. Mice were revived using antisedan (atipamezole, 0.5 mg/kg I.P.) and treated with ketoprofen (5 mg/kg I.P.) for 3 days post-operatively. ChR2 expression and anatomical specificity were validated empirically according (a) to the expression of eYFP in the medial PFC and paraventricular region of the MDT and (b) high-fidelity AMPAR-mediated oEPSCs in NAc D1(+) and D1(-) MSNs.

Intra-NAc Microinfusions

Bilateral guide cannulas (26 gauge, cut to 3 mm length, 2mm center to center distance, C235GS-5-2.0/SPC- Plastics One, 22 Roanoke VA) were ventral to the NAc core (AP: 1.45, ML: ±1.00, DV: 3.00). Infusion guides were secured into place using dental cement and fitted with a dummy cannula (C235DCS-5/SPC, Plastics One, Roanoke VA) and dust cap (303DC/1 Plastics One, Roanoke VA). Animals were allowed to recover for at least 5 days before experimentation. Prior to exposure to the AIS paradigm, bilateral infusion cannulae (4mm cut length; C235IS-5/SPC, Plastics One, Roanoke VA) were connected to a 1 uL syringe (#7001, Hamilton Company, Reno, NV) by polyethylene tubing (0.46 mm in diameter; Plastics One). H_3R antagonist, JNJ 5207852, was infused at a dose of 0 (saline, vehicle) or 3.89 µg/µL at rate of 0.4 µL over 60-sec and was allowed to absorb for 90-sec before cannula was removed. Animals were then permitted 5-min prior to entering the immobilization apparatus.

Pharmacology

Histamine dihydrochloride, thioperamide, JNJ 5207852, cetirizine hydrochloride, ranitidine hydrochloride, *(R)*-(-)-α-methylhistamine dihydrobromide, RuBi-Glutamate, (*RS*)-baclofen, Akti$_{1/2}$, CHIR 99021, gallein, forskolin, NBQX, picrotoxin, and H89 dihydrochloride were each purchased from Tocris Biosciences.

Statistics and Data Analysis

Electrophysiological experiments were analyzed using Clampfit 10.4 and GraphPad Prism v7.0. Changes in baseline EPSC (electric or optically-evoked) amplitude, coefficient of variance (CV), and PPR were calculated by comparing mean values during 5 min intervals specified in each time-course to baseline PPR and CV values. A depression was defined as a significant difference in e/oEPSC amplitude from baseline calculated during the time interval specified in the recording. AP probability was assessed by calculating the percentage of APs evoked following each stimulus train. Gain was calculated by the slope of a linear regression function fitted to the AP probability quantified during each stimulus frequency. After obtaining each data set, Shapiro-Wilk tests were performed to assess normality. Data depicted in Figures 1-7 (and S1-S2) were determined to be normally distributed. Thus, paired or unpaired *t*-tests were used to analyze statistical differences between data sets. Sidak's post-hoc analyses were used for analyses requiring multiple comparisons. Power analyses were performed with preliminary data during the acquisition of each new data set. The sample size obtained from each power analysis calculation was then compared to sample sizes reported in the literature for similar experiments. Errors bars depicted in figures represent SEM. For all analyses, α was set as 0.05, with P values $< \alpha$ indicating a statistically significant difference.